Published in final edited form as:
Cancer Discov. 2014 May ; 4(5): 554–563. doi:10.1158/2159-8290.CD-13-0929.

A diverse array of cancer-associated mTOR mutations are hyperactivating and can predict rapamycin sensitivity

Brian C. Grabiner[1,2,3,4], **Valentina Nardi**[5], **Kivanc Birsoy**[1,2,3,4], **Richard Possemato**[1,2,3,4], **Kuang Shen**[1,2,3,4], **Sumi Sinha**[1], **Alexander Jordan**[1], **Andrew H. Beck**[6], and **David M. Sabatini**[1,2,3,4]

[1]Whitehead Institute for Biomedical Research, Cambridge, MA 02142

[2]Howard Hughes Medical Institute and Department of Biology, MIT, Cambridge, MA 02139

[3]Broad Institute of Harvard and MIT, Cambridge, MA 02142

[4]The David H. Koch Institute for Integrative Cancer Research at MIT, Cambridge, MA 02139

[5]Department of Pathology and Massachusetts General Hospital Cancer Center, Boston, MA 02114

[6]Department of Pathology, Beth Israel Deaconess Medical Center and Harvard Medical School, Boston, MA 02215

Abstract

Genes encoding components of the PI3K-Akt-mTOR signaling axis are frequently mutated in cancer, but few mutations have been characterized in *MTOR*, the gene for the mTOR kinase. Using publicly available tumor genome sequencing data, we generated a comprehensive catalog of mTOR pathway mutations in cancer, identifying 33 *MTOR* mutations that confer pathway hyperactivation. The mutations cluster in six distinct regions in the C-terminal half of mTOR and occur in multiple cancer types, with one cluster particularly prominent in kidney cancer. The activating mutations do not affect mTOR complex assembly, but a subset reduces binding to the mTOR inhibitor Deptor. mTORC1 signaling in cells expressing various activating mutations remains sensitive to pharmacological mTOR inhibition, but is partially resistant to nutrient deprivation. Lastly, cancer cell lines with hyperactivating *MTOR* mutations display heightened sensitivity to rapamycin both in culture and as *in vivo* xenografts, suggesting that such mutations confer mTOR pathway dependency.

Keywords

personalized; mTOR; mutations; biomarker; deptor

Corresponding author David M. Sabatini Professor of Biology, MIT Investigator, Howard Hughes Medical Institute Senior Associate Member, Broad Institute Member, Koch Institute for Cancer Research at MIT Nine Cambridge Center Cambridge, Massachusetts 02142 617-258-6407 / fax 617-452-3566 sabatini@wi.mit.edu.

Conflict of interest
The authors have no conflicts of interest to declare.

Introduction

In mammals, the PI3K-Akt-mTOR pathway regulates cell size, mRNA translation, autophagy and many metabolic processes, including lipid synthesis (1). A variety of upstream regulators control the activity of the serine/threonine protein kinase mTOR and many of these are deregulated in cancer, resulting in pathway hyperactivation. Such activation occurs most commonly through loss-of-function mutations in tumor suppressors, such as phosphatase and tensin homolog (*PTEN*), tuberous sclerosis 1/2 (*TSC1/2*), neurofibromin 1/2 (*NF1/2*), or oncogenic mutations in *KRAS*, *PIK3CA*, or *AKT* (2). However, few cancer-associated mutations have been functionally characterized in *MTOR* itself, with only two reports thus far describing such mutations. In the first report, the authors tested six cancer-associated *MTOR* mutations and observed that two (S2215Y from a colorectal sample and R2505P from a kidney sample) conferred mTOR complex 1 (mTORC1) activation (3). In the second report, the authors identified an mTORC1 activating *MTOR* mutation (L2431P) that was present in a portion but not the entirety of a primary kidney tumor (4). Although these initial reports establish that activating *MTOR* mutations do arise in cancer, they were based upon limited sample sets that do not reflect the diverse subtypes of cancer. More recently, cancer genome sequencing projects, such as The Cancer Genome Atlas (TCGA) and the Cancer Cell Line Encyclopedia (CCLE), have identified a vast number of somatic mutations in thousands of tumors from more than 40 cancer subtypes (5-7).

Using publicly available databases of cancer genome sequence data, we cataloged all mutations in mTOR pathway components. We annotated over 400 samples with missense mutations in the *MTOR* gene from dozens of cancer subtypes, most of which lie within six clusters in the part of the gene that encodes the C-terminal portion of mTOR. Furthermore, through functional analyses, we identify 33 novel mTOR pathway-activating mutations, some of which affect the capacity of mTOR to interact with its partner proteins. None of the activating mutations impact the sensitivity of mTORC1 activity in cells to mTOR inhibitors but a subset confer mTORC1 signaling resistance to nutrient deprivation. Importantly, cancer cells that naturally express a subset of the mutations are hypersensitive to the mTOR inhibitor rapamycin. These findings may have translational relevance as rapamycin analogs (rapalogs) are clinically approved for the treatment of cancer, and several ATP-competitive mTOR kinase inhibitors are in development (8). As tumor biopsies are increasingly subjected to whole exome sequencing, the hyperactivating *MTOR* mutations we characterize may serve as biomarkers in predicting cancer response to mTOR-targeting drugs.

Results

Catalog of recurring mutations in genes encoding mTOR pathway components

To generate a comprehensive catalog of all cancer-associated missense mutations in canonical genes of the mTOR pathway, we analyzed partial genome sequencing data from the TCGA, CCLE, International Cancer Genome Consortium (ICGC) and Catalogue of Somatic Mutations in Cancer (COSMIC) databases (5-7, 9, 10). This analysis revealed that almost every gene in the mTOR pathway harbored somatic point mutations (Supplementary Table 1). To enrich for mutations that are more likely to affect pathway function, only

mutations that alter the same codon more than once were counted. When normalized for gene length, this analysis revealed that *MTOR* contained the highest percentage of recurring mutations, and thus we focused most of our attention on these mutations (Supplementary Figure 1). Collectively, through data mining and a literature search, we curated over 400 samples with non-synonymous *MTOR* point mutations (Figure 1B and Supplementary Table 2) (11-17). While the majority of these mutations are represented by only one sample in our database, approximately 40% are recurrent, most of which have not been previously described. Additionally, the mutations cluster in six distinct regions of mTOR centered on highly recurrent mutations that alter amino acids C1483, E1799, T1977, S2215, L2427 and R2505 (Figure 1C). The presence of these clusters suggests that there is a selective advantage to acquiring mutations in certain regions of the mTOR protein. Furthermore, these mutations are present in multiple cancer subtypes, with the highest number in colorectal, endometrial, and lung cancers, although these cancer subtypes are also considered to have the highest mutation rates (Figures 1D and 1E) (18). Interestingly, a random mutagenesis screen in the *S. pombe* mTOR homolog (*tor2*) identified activating mutations in homologous amino acid positions to many of those we find in *MTOR* to be recurrently mutated in cancer (19) (Supplementary Table 3).

mTORC1/2 activating mutations in *MTOR*

The prevalence of the recurrent mutations, their clustering, and correlation with activating *tor2* mutations strongly suggested that the *MTOR* mutations impact mTOR pathway activity. To test this possibility, wild-type (WT) or ten different mutants of mTOR (L1460P, C1483F, E1799K, F1888L, T1977R, V2006I, S2215Y, I2500F, R2505P, and D2512H) were expressed in cells and phosphorylation of the mTORC1/2 substrates S6K1, 4EBP1, or Akt1 examined (Figures 2A, 2B, and 2C). All the mTOR mutants conferred varying degrees of pathway activation, and, interestingly, a few displayed some substrate preference (L1460P, C1483F, S2215Y, and R2505P towards S6K1/4EBP1 or V2006I towards Akt1), implying that these mutations have greater effects on mTORC1 or mTORC2. Thus, while three pathway activating *MTOR* mutations have previously been identified (3, 4), our initial analyses uncovered an additional eight recurrent *MTOR* mutations which activate mTORC1 and/or mTORC2.

It is well established that two activating mutations (E545K and H1047R) within the phosphatidylinositol-4,5-bisphosphate 3-kinase, catalytic subunit alpha (PI3K-p110α), encoded by the *PIK3CA* gene, can lead to mTOR pathway activation (20). To determine the degree of mTOR pathway activation conferred by mTOR mutation, S6K1 phosphorylation from cells expressing WT or S2215Y mTOR was compared to cells expressing WT or mutant PI3K-p110α (Supplementary Figures 2A and 2B). This revealed that while expression of only mutant mTOR conferred mTORC1 activation, expression of either WT or mutant PI3K-p110α induced mTORC1 activity.

Non-recurrent *MTOR* mutations that activate mTORC1 signaling

We next examined in more detail the nature of the activating *MTOR* mutations, and observed that while some codons are mutated to only one other residue (e.g. E1799K), others are mutated to several different amino acids (e.g. S2215F/P/T/Y). This is reminiscent

of the diverse amino acids to which the G12 residue of *KRAS* is mutated in cancers (21). We expressed 20 such *MTOR* mutations and found that many (C1483R/W/Y, F1888I, T1977K, S2215F/P, I2500M), but not all (A41P/S/T, F1888V, T1977S, V2006L, S2215T, R2505Q/*, D2512G/Y), led to increased S6K1 phosphorylation (Supplementary Figures 3 and 5, and data not shown). Given that most of these activating mutations are found only once in our dataset implies that other non-recurrent mutations may also activate mTORC1 signaling. To identify other such mutations, we turned our attention to the mutational clusters identified in Figure 1, and observed that while most are represented by several tissue types, those in the C1483 cluster are particularly prevalent in kidney cancer (Figure 1E and Supplementary Figure 3D). Interestingly, two recent cancer genome sequencing efforts reported that kidney cancers have an increased percentage of mutations in mTOR pathway genes, but the functional consequences of these mutations were not evaluated (13, 22). Expression of the ten kidney cancer-associated *MTOR* mutations from the C1483 cluster revealed that in addition to the previously evaluated L1460P and C1483F/Y mutants (Figure 1B and Supplemental Figure 2), three non-recurrent mutants (L1433S, A1459P, and E1519T) also induced mTORC1 pathway activity (Figure 2D). Similarly, expression of eight non-recurrent mutations from the S2215 cluster (N2206S, L2209V, A2210P, L2216P, R2217W, L2220F, Q2223K, and A2226S) activated mTORC1 signaling as measured by S6K1 phosphorylation, with the L2209V mutant conferring higher activation than even S2215Y (Supplementary Figure 3E). Lastly, other than the S2215Y and R2505P mutations, the only other cancer-associated *MTOR* mutation previously characterized is L2431P from a kidney cancer patient (4). Expression of mTOR containing this non-recurrent mutation caused mTORC1 activation that was much weaker than that caused by expression of the S2215Y mutant (Supplementary Figure 3F). Collectively, these results suggest that while most non-recurrent *MTOR* mutations found in cancer are part of the mutational “noise”, there exists a diverse set of *MTOR* mutations that can drive mTORC1 pathway activity. Likely, as more cancer genomes are sequenced, the activating non-recurrent mutations we identified will prove to be recurrent.

Recurrent mutations in *RHEB* activate mTORC1

We also observed that other mTOR pathway genes such as Raptor, Rictor, and Rheb1 harbored recurrent mutations (Supplemental Table 1). Expression of Rheb1 Y35N/C/H and to a lesser degree E139K increased phosphorylation of endogenous S6K1 more than that of WT Rheb1 (Figure 2E), while recurrent mutations in Raptor (R788C) or Rictor (S1101L) failed to induce any mTORC1 or mTORC2 activity (data not shown). In support of the relevance of these mutations to cancer, *RHEB* was recently highlighted as a novel cancer gene due to the presence of the Y35N mutation (23). Thus, cancer associated mutations in either *MTOR* or *RHEB* can induce mTORC1 activity; whether this is true of other mTOR pathway genes remains to be determined.

mTORC1/2 hyperactivating mutants bind less Deptor

One potential mechanism through which the mutations in mTOR (Figure 2) might increase S6K1/Akt1 phosphorylation is by altering mTORC1 or mTORC2 assembly. Alternatively or in addition, the mTOR mutations may diminish the binding of mTOR to its endogenous inhibitor Deptor, which binds to the FAT domain of mTOR (24). To test these possibilities,

the interactions of exogenously expressed WT or mutant mTORs with endogenous Raptor, Rictor, and Deptor were measured. All mutant mTOR proteins bound equally well to Raptor and Rictor, suggesting that the mutations do not affect formation of either mTOR complex (Figure 3A). In contrast, Deptor binding to the immunoprecipitated mTOR proteins was reduced in cells expressing the mTOR mutants as compared to WT mTOR (Figure 3A). Given that increased mTOR pathway activity correlates with a reduction in the mTOR-Deptor interaction (24), it is likely that the observed decrease in Deptor binding reflects the increased mTOR pathway activity caused by the *MTOR* mutations. However, two mTORC1 activating mutations that are in the FAT domain of mTOR, L1460P and C1483Y, bound much less Deptor than the other mutants tested (Figure 3A), suggesting that these mutations directly perturb the Deptor binding site on mTOR. Consistent with this, examination of the mutations from the C1483 cluster described in figure 2D revealed that two other highly activating mutations in the FAT domain (A1459P and C1483Y) also strongly reduced the mTOR-Deptor interaction (Supplementary Figure 4A). While these results suggest a possible mechanism of action for a subset of activating mTOR mutations, they do not preclude other mechanism by which *MTOR* mutations may impact mTORC1 signaling, such as by increasing the activity of the mTOR kinase domain.

MTOR mutations do not affect mTORC1 sensitivity to mTOR inhibitors but can affect the pathway response to nutrient deprivation

We next considered the possibility that the mTORC1-activating *MTOR* mutants have altered sensitivity to established mTOR inhibitors. Engineered mutations in the FRB domain of mTOR, which binds the FKBP12-rapamycin complex, confer marked rapamycin resistance to mTOR (25). To test whether mTOR mutation alters pathway inhibition by rapamycin or Torin1 (an investigational ATP-competitive mTOR inhibitor), we used HEK-293 cells with an integrated FLP recombination site (TREX cells) to stably express WT or several different mutants of mTOR (A1459P, C1483Y, E1799K, F1888I, L2209V, S2215Y, L2431P, I2500F, and R2505P), as the mTOR cDNA is too large to be packaged and expressed via a lentiviral delivery system (Supplementary Figure 4B). Baseline phosphorylation of endogenous S6K1 was higher in TREX cells expressing the A1459P, L2209V, S2215Y, I2500F and R2505P mTOR mutants than in parental or WT-expressing cells (Figure 3B and Supplementary Figures 4C and 4D), consistent with the results obtained upon transient expression of these mutants (Figures 2A and 2D, and Supplementary Figure 3D). Importantly, mTORC1 activity in none of the TREX cells was resistant to rapamycin, Torin1, MLN0128 (an mTOR ATP-competitive inhibitor), GDC0980 (a dual PI3K/mTOR ATP-competitive inhibitor), (Figure 3B and Supplementary Figures 4C and 4D). Thus, on a molecular level, while cells with mTOR mutations may display high levels of mTORC1/2 activity, this activity is still sensitive to pharmacological mTOR inhibition.

The kinase activity of mTOR is tightly regulated by nutrient availability; when cells are starved of nutrients (specifically glucose and amino acids), they downregulate mTORC1 signaling, while retreatment of cells with these nutrients restores mTORC1-mediated signaling (26). Given this, we sought to determine whether any of the activating mTOR mutants affect the sensitivity of mTORC1 signaling to amino acid or glucose withdrawal. Indeed, S6K1 phosphorylation was highly resistant to deprivation of either nutrient in cells

expressing several mutants (A1459P, S2215Y, I2500F and R2505P) (Figure 3C and Supplementary Figures 4E and 4F). This observation may be relevant in the context of developing tumors, which are often glucose starved (27, 28), where inappropriate mTORC1 activity may provide a growth advantage.

Cancer cells with hyperactivating *MTOR* mutations are hypersensitive to rapamycin *in vitro* and *in vivo*

To determine if cancer cells with *MTOR* mutations are dependent on mTORC1 activity, we evaluated the impact of rapamycin on the proliferation of set of cancer cell lines harboring WT or mutant mTOR (Figure 4A). We identified four cell lines with mTORC1-activating *MTOR* mutations (C1483Y in MOLT16; E1799K in HEC59 and SNU349; and S2215Y in JHUEM7) and two with *MTOR* mutations that have no apparent impact on mTORC1 signaling (V2006L in TUHR10TKB; and R2152C in A375) (Supplementary Figures 5A and 5B). HeLa cells were used as a negative control cell line, as they are mildly rapamycin sensitive and are wild-type for mTOR (7, 29). MCF7 and SW780 cells, which are also wild-type for mTOR, served as positive controls for rapamycin sensitivity because the MCF7 cells harbor an activating PI3K-p110α mutation (E545K) while the SW780 cells lack *NPRL2*, which encodes a component of the GATOR1 negative regulator of the amino acid-sensing pathway (30, 31). Importantly, only the cell lines with activating *MTOR* mutations, the PI3K-p110α mutant, or the NPRL2-null SW780 cells were hypersensitive to rapamycin treatment (Figure 4B). Consistent with these and published results, the growth of HeLa xenografts was partially rapamycin sensitive, while rapamycin completely halted the growth of HEC59 xenografts, which carry the hyperactivating mTOR E1799K mutation (Figure 4C) (32, 33). These results suggest that the presence of hyperactivating *MTOR* mutations in cancer cells may serve as biomarkers to identify tumors that are likely to respond to mTOR inhibitors.

Discussion

Early cancer genome sequencing projects led to the identification of three mutations in *MTOR* that were shown to activate mTORC1 signaling (3, 4). Here, we have identified an additional 33 previously unknown activating *MTOR* mutations (some are recurrent, others are not) (Supplementary Table 4). Mechanistically, we find that the activating mutations diminish the mTOR-Deptor interaction and interestingly, when mapped onto the recently solved crystal structure of mTOR, the mutations cluster in several distinct locations within the protein itself, suggesting that other activating mechanisms may exist (Supplementary Figure 6) (34). While the mutations do not prevent pharmacological mTOR inhibition, a subset protect against the effects of nutrient deprivation on mTORC1 signaling. Lastly, we demonstrate that cell lines with activating *MTOR* mutations are particularly sensitive to rapamycin in cell culture and in xenografts, likely due to mTOR pathway dependency.

The diversity of activating *MTOR* mutations we characterized is reminiscent of the various activating mutations in the prototypical lipid kinase *PIK3CA*, which encodes for the PI3K catalytic subunit p110α (35). However, unlike the activating *PIK3CA* mutations, which confer equal activation of PI3K-mediated signaling pathways, the diverse *MTOR* mutations

can differentially activate mTORC1 or mTORC2, leading to either S6K1/4EBP1 or Akt1 phosphorylation, respectively. This finding is particularly relevant in a clinical setting, as patients with mTORC1 activating mutations may respond well to FDA-approved rapalogs, while patients with mTORC2 activating mutations might best be treated with ATP-competitive mTOR inhibitors, although such inhibitors are still in clinical trials. This distinction is especially relevant for patients with mTORC2 activating mutations, because rapalogs can in some cases upregulate mTORC2 signaling through modulation of an mTORC1-dependent feedback loop (36).

Rapalog-based therapies are currently approved or in clinical trials for several cancer subtypes, and some patients have had dramatic and durable responses to these therapies (37). Given that some cells with activating *MTOR* mutations are particularly rapamycin sensitive (Figure 4), it is possible that some of the rapalog-responsive patients had tumors with similar mutations. Indeed, it was recently found that the tumor of a bladder cancer patient with two activating *MTOR* mutations displayed exquisite sensitivity to rapalog-based therapy (38). Many more cancer-associated *MTOR* mutations will likely be identified in future studies, but functional evaluation of these mutations will be required to determine their impact on the mTOR pathway. As tumor sequencing becomes more commonplace, functional studies such as ours may aid in arriving at a more personalized treatment regimen that eventually promotes patient survival.

Methods

Data acquisition and cluster analysis

All mutations in genes of the mTOR pathway were acquired from the cBIO, COSMIC, and ICGC databases or through a literature search with a data-freeze date of September 1, 2013. To identify regions of mTOR significantly enriched for somatic point mutations, we determined the probability of seeing at least the observed number of mutations in a 50 amino acid sliding window with the null hypothesis being all 463 *MTOR* mutations randomly occurring across the 2549 amino acid protein. Specifically, we calculated a threshold for significance of at least 15 mutations per 50 amino acids by the formula:

$$\mathrm{p}=\sum_{n=k}^{463}\left(\begin{array}{c}463\\k\end{array}\right)*\left(1-\frac{50}{2549}\right)^{463-k}*\left(\frac{50}{2549}\right)^{k}$$

which equals 0.043 for k = at least 15 mutations per 50 amino acids.

Materials

Reagents were obtained from the following sources: antibodies to HA (clone C29F4), S6K1 (clone 49D7), phospho-T389-S6K1 (clone 108D2), and phospho-S473-Akt1 (clone D9E) from Cell Signaling Technology; antibody to GAPDH (clone GT239) from Genetex; antibodies to Deptor and Raptor, X-ray film, and PVDF membrane were from Millipore; antibody to Rictor from Bethyl; antibody to the Flag epitope (clone M2), Flag M2-coupled agarose beads, glucose and amino acid mixtures from Sigma; horseradish-peroxidase-labeled anti-mouse and anti-rabbit secondary antibodies from Santa Cruz Biotechnology;

FuGENE HD and Cell Titer Glo from Promega; X-tremeGENE 9 and Complete Protease Mixture from Roche Applied Science; QuikChange II XL from Stratagene; enhanced chemiluminescence reagent and glutathione-coupled agarose beads from Thermo; 8-week-old nude mice from Taconic; rapamycin from LC Labs; MLN0128 and GDC0980 from Selleckchem; and Torin1 was synthesized in the Gray laboratory (39). cDNAs for mTOR and PI3K-p110α were from Addgene; expression vectors for HAGST-S6K1, HA-GST-Akt1, and HA-GST-Rheb1 were described previously (24, 40, 41) and Flag-14-3-3α was a generous gift from the Yaffe lab. The primers used to generate the mTOR and Rheb1 mutations were from Integrated DNA Technologies and are listed in supplemental table 5. HEK-293T-TREX cell system, 4-12% bis-tris SDS-PAGE gels, and 20x MOPS buffers were from Invitrogen.

Tissue culture and cell lines

MCF7, HELA, HEK-293T, HCT116, A375 and SW780 cells were from ATCC; JHUEM7, MOLT16, NCIH446, SNU349, and TUHR10TKB cells were from the Broad Institute Cancer Cell Line Encyclopedia; HEK-293E cells were a generous gift of the Blenis lab; and the HEC59 cells were a generous gift of the Lippard lab. The cell lines have not been re-authenticated, although those from ATCC and the Broad were used within 6 months of resuscitation. The HEK-293T, HEK-293E, HCT116, A375, HEC59, and TUHR10TKB cells were cultured in DMEM; JHUEM7 and MOLT16 cells were cultured in RPMI; and the SW780 cells were cultured in IMDM. All media was prepared with 10% heat inactivated FBS and 1% Penicillin/Streptomycin. All cell lines were maintained at 37°C, 5% CO_2.

Site-directed mutagenesis, cloning, and TREX cell line generation

All *MTOR* and *RHEB* point mutations were generated in the parental vectors using site-directed mutagenesis with the QuikChange II XL kit according to the manufacturer's protocol. Primer sequences are listed in Supplementary Table 5. Point mutations were verified using Sanger sequencing as conducted by Eton Biosciences. The HA-GST-4EBP1 reporter vector was generated by synthesizing a gBlock from IDT encoding for 4EBP1 and cloning it into the pRK5-HA-GST vector using SalI and NotI restriction digestion followed by ligation. WT and mutant mTOR cDNAs were subcloned directly from the pcDNA3 vector into the pcDNA5/FRT/TO vector using single site NotI restriction digestion followed by ligation. Flag-mTOR-expressing TREX cells were generated according to the manufacturer's protocol.

Cell treatments, lysis, and immunoprecipitations

For S6K1 and Akt1 co-transfection assays, 3×10^5 HEK-293T or HEK-293E cells per well were seeded into 6-well tissue culture plates, transfected 24 hours later with 2 μg of mTOR-encoding plasmid and 1 ng of S6K1- or Akt1-encoding plasmid using X-tremeGENE 9 or FuGENE HD, followed by whole cell lysis 48 hours after transfection in NP-40 lysis buffer (50 mM Tris-HCl at pH 7.5, 150 mM NaCl, 1% NP-40 substitute, 1 mM EDTA at pH8.0, 50 mM NaF, 10 mM Na-pyrophosphate, 15 mM Na_3VO_4, 100 mM β-glycerophosphate, and 1 tablet of protease inhibitor per 50 mL of buffer). 200-400 μg of whole cell lysates were mixed with 5x SDS-sample buffer to a final concentration of 1-2 μg/μL, boiled for 5

minutes, and then used directly for immunoblotting or frozen at −20°C. For glutathione pull down assays, 2×10^6 HEK-293T cells were seeded onto 10 cm tissue culture plates, transfected 24 hours later with 10 μg of mTOR-encoding plasmid and 2 ng of S6K1-encoding plasmid using X-tremeGENE 9, and lysed 48-72 hours after transfection in NP-40 lysis buffer. 2-3 mg of the resultant whole-cell lysates were incubated with 30 μL of pre-washed glutathione-coupled agarose beads in a 1 mL volume, which were rotated at 4°C for two hours, spun at 2,500 RCF for one minute, washed in 500 μL lysis buffer three times, and the beads directly boiled in 50 μL of 2x SDS-sample buffer. For mTOR immunoprecipitations, the cells were treated as with the glutathione pulldown, except they were lysed/washed in CHAPS buffer (50 mM HEPES at pH 7.4, 150 mM NaCl, 0.4% CHAPS, 50 mM NaF, 10 mM Na-pyrophosphate, 100 mM β-glycerophosphate, and 1 tablet of protease inhibitor per 50 mL of buffer) and incubated with Flag-M2-coupled agarose beads.

Immunoblotting

10-50 μg of whole cell lysates, 10-30 μL of glutathione pulldown samples, or 10-30 μL of Flag-M2 immunoprecipitates were loaded into lanes of 4-12% bis-tris SDS-PAGE gels, run at 120 volts for 2 hours in 1x MOPS buffer, and then transferred to 0.45 μm PVDF membrane at 60 volts for 2 hours in 1x transfer buffer (100 mM CAPS, 123 mM NaOH, 10% Ethanol). The membranes were then immunoblotted for the indicated proteins. All primary antibodies were diluted 1:1000 in 5% BSA W/V TBST, with the exception of GAPDH and Flag antibodies which were diluted 1:2000. All secondary antibodies were diluted 1:5000 in 5% milk W/V TBST. Densitometry was performed using ImageJ and a student's T test was used to determine statistical significance.

Rapamycin, Torin1, MLN0128, GDC0980, and nutrient starvation/re-stimulation treatments

For the mTOR inhibitor experiments, 3×10^5 TREX cells per well were seeded into 6-well plates, grown for one day, treated with 100 nM rapamycin, 250 nM Torin1, 250 nM MLN0128, 250 nM GDC0980, or DMSO for 60 minutes. The cells were then lysed as above. For the nutrient deprivation experiments, 3×10^5 TREX cells per well were seeded into 6-well plates, grown for one day, rinsed briefly in 1x amino acid- or glucose-free RPMI, incubated in 1x amino acid- or glucose-free RPMI for 60 minutes, and then stimulated with free amino acids or glucose to the levels in complete RPMI for 15 minutes.

In vitro proliferation assays

Six replicates each of 800-1200 cells were seeded into 96-well plates, treated with 8 doses of rapamycin 24 hours later, and assayed for ATP content using Cell Titer Glo 96 hours following rapamycin treatment according to the manufacturer's protocol.

In vivo xenograft assays

3×10^6 cells per injection site were implanted subcutaneously into the right and left flanks of nude mice. Once tumors were palpable in all animals (>50 mm^3 volume by caliper measurements), mice were assigned randomly into rapamycin treated or untreated groups and caliper measurements were taken every 3-4 days until tumor burden approached the

limits set by institutional guidelines. Tumor volume was assessed according to the formula (0.5)(W)(W)(L), and a student's T test was used to determine the p-values. Rapamycin (4 mg/kg) or vehicle was delivered by daily IP injection, 100 mL per injection. All experiments involving mice were carried out with approval from the Committee for Animal Care at MIT and under supervision of the Department of Comparative Medicine at MIT.

Supplementary Material

Refer to Web version on PubMed Central for supplementary material.

Acknowledgments

The authors would like to thank N. Wagle and L. Garraway for providing whole exome sequencing data from a renal cell carcinoma patient who harbored an *MTOR* missense mutation.

Financial Support

This research is supported in part by a Postdoctoral Fellowship (#118855-PF-10-069-01-TBG) from The American Cancer Society to B.G., The Leukemia and Lymphoma Society and The Jane Coffin Childs Fund to K.B., and grants from the Starr Cancer Consortium, David H. Koch Institute for Integrative Cancer Research at MIT, The Alexander and Margaret Stewart Trust Fund, and NIH (K99 CA168940 to R.P. and CA103866, CA129105, and AI07389 to D.M.S.). D.M.S. is an investigator of the Howard Hughes Medical Institute

Abbreviations

mTOR	mechanistic Target of Rapamycin
PI3K	phosphatidylinositol-4,5-bisphosphate 3-kinase
mTORC	mTOR complex

References

1. Laplante M, Sabatini DM. mTOR signaling in growth control and disease. Cell. 2012; 149(2):274–93. Epub 2012/04/17. doi: S0092-8674(12)00351-0 [pii] 10.1016/j.cell.2012.03.017. PubMed PMID: 22500797; PubMed Central PMCID: PMC3331679. [PubMed: 22500797]
2. Zoncu R, Efeyan A, Sabatini DM. mTOR: from growth signal integration to cancer, diabetes and ageing. Nat Rev Mol Cell Biol. 12(1):21–35. Epub 2010/12/16. doi: nrm3025 [pii] 10.1038/nrm3025. PubMed PMID: 21157483; PubMed Central PMCID: PMC3390257. [PubMed: 21157483]
3. Sato T, Nakashima A, Guo L, Coffman K, Tamanoi F. Single amino-acid changes that confer constitutive activation of mTOR are discovered in human cancer. Oncogene. 2010; 29(18):2746–52. Epub 2010/03/02. doi: 10.1038/onc.2010.28. PubMed PMID: 20190810; PubMed Central PMCID: PMC2953941. [PubMed: 20190810]
4. Gerlinger M, Rowan AJ, Horswell S, Larkin J, Endesfelder D, Gronroos E, et al. Intratumor heterogeneity and branched evolution revealed by multiregion sequencing. N Engl J Med. 2012; 366(10):883–92. Epub 2012/03/09. doi: 10.1056/NEJMoa1113205. PubMed PMID: 22397650. [PubMed: 22397650]
5. Cerami E, Gao J, Dogrusoz U, Gross BE, Sumer SO, Aksoy BA, et al. The cBio cancer genomics portal: an open platform for exploring multidimensional cancer genomics data. Cancer Discov. 2(5): 401–4. Epub 2012/05/17. doi: 2/5/401 [pii] 10.1158/2159-8290.CD-12-0095. PubMed PMID: 22588877. [PubMed: 22588877]
6. Gao J, Aksoy BA, Dogrusoz U, Dresdner G, Gross B, Sumer SO, et al. Integrative analysis of complex cancer genomics and clinical profiles using the cBioPortal. Sci Signal. 6(269):pl1. Epub

2013/04/04. doi: scisignal.2004088 [pii] 10.1126/scisignal.2004088. PubMed PMID: 23550210. [PubMed: 23550210]

7. Barretina J, Caponigro G, Stransky N, Venkatesan K, Margolin AA, Kim S, et al. The Cancer Cell Line Encyclopedia enables predictive modelling of anticancer drug sensitivity. Nature. 483(7391): 603–7. Epub 2012/03/31. doi: nature11003 [pii] 10.1038/nature11003. PubMed PMID: 22460905; PubMed Central PMCID: PMC3320027. [PubMed: 22460905]
8. Benjamin D, Colombi M, Moroni C, Hall MN. Rapamycin passes the torch: a new generation of mTOR inhibitors. Nat Rev Drug Discov. 10(11):868–80. Epub 2011/11/01. doi: nrd3531 [pii] 10.1038/nrd3531. PubMed PMID: 22037041. [PubMed: 22037041]
9. Forbes SA, Bindal N, Bamford S, Cole C, Kok CY, Beare D, et al. COSMIC: mining complete cancer genomes in the Catalogue of Somatic Mutations in Cancer. Nucleic Acids Res. 39(Database issue):D945–50. Epub 2010/10/19. doi: gkq929 [pii] 10.1093/nar/gkq929. PubMed PMID: 20952405; PubMed Central PMCID: PMC3013785. [PubMed: 20952405]
10. Hudson TJ, Anderson W, Artez A, Barker AD, Bell C, Bernabe RR, et al. International network of cancer genome projects. Nature. 464(7291):993–8. Epub 2010/04/16. doi: nature08987 [pii] 10.1038/nature08987. PubMed PMID: 20393554; PubMed Central PMCID: PMC2902243. [PubMed: 20393554]
11. Brastianos PK, Horowitz PM, Santagata S, Jones RT, McKenna A, Getz G, et al. Genomic sequencing of meningiomas identifies oncogenic SMO and AKT1 mutations. Nat Genet. 45(3): 285–9. Epub 2013/01/22. doi: ng.2526 [pii] 10.1038/ng.2526. PubMed PMID: 23334667; PubMed Central PMCID: PMC3739288. [PubMed: 23334667]
12. Kasaian K, Wiseman SM, Thiessen N, Mungall KL, Corbett RD, Qian JQ, et al. Complete genomic landscape of a recurring sporadic parathyroid carcinoma. J Pathol. 230(3):249–60. Epub 2013/04/26. doi: 10.1002/path.4203. PubMed PMID: 23616356. [PubMed: 23616356]
13. Sato Y, Yoshizato T, Shiraishi Y, Maekawa S, Okuno Y, Kamura T, et al. Integrated molecular analysis of clear-cell renal cell carcinoma. Nat Genet. 45(8):860–7. Epub 2013/06/26. doi: ng.2699 [pii] 10.1038/ng.2699. PubMed PMID: 23797736. [PubMed: 23797736]
14. Lee JH, Huynh M, Silhavy JL, Kim S, Dixon-Salazar T, Heiberg A, et al. De novo somatic mutations in components of the PI3K-AKT3-mTOR pathway cause hemimegalencephaly. Nat Genet. 44(8):941–5. Epub 2012/06/26. doi: ng.2329 [pii] 10.1038/ng.2329. PubMed PMID: 22729223. [PubMed: 22729223]
15. Shull AY, Latham-Schwark A, Ramasamy P, Leskoske K, Oroian D, Birtwistle MR, et al. Novel somatic mutations to PI3K pathway genes in metastatic melanoma. PLoS One. 7(8):e43369. Epub 2012/08/23. doi: 10.1371/journal.pone.0043369 PONE-D-12-14005 [pii]. PubMed PMID: 22912864; PubMed Central PMCID: PMC3422312. [PubMed: 22912864]
16. Zhang J, Grubor V, Love CL, Banerjee A, Richards KL, Mieczkowski PA, et al. Genetic heterogeneity of diffuse large B-cell lymphoma. Proc Natl Acad Sci U S A. 110(4):1398–403. Epub 2013/01/08. doi: 1205299110 [pii] 10.1073/pnas.1205299110. PubMed PMID: 23292937; PubMed Central PMCID: PMC3557051. [PubMed: 23292937]
17. Smith LD, Saunders CJ, Dinwiddie DL, Atherton AM, Miller NA, Soden SE, et al. Exome Sequencing Reveals De Novo Germline Mutation of the Mammalian Target of Rapamycin (MTOR) in a Patient with Megalencephaly and Intractable Seizures. Journal of Genomes and Exomes. 2:63–72. 3863-JGEExome-Sequencing-Reveals-De-Novo-Germline-Mutation-of-the-Mammalian-Ta.pdf doi: 10.4137/jge.s12583.
18. Alexandrov LB, Nik-Zainal S, Wedge DC, Aparicio SA, Behjati S, Biankin AV, et al. Signatures of mutational processes in human cancer. Nature. 500(7463):415–21. Epub 2013/08/16. doi: nature12477 [pii] 10.1038/nature12477. PubMed PMID: 23945592; PubMed Central PMCID: PMC3776390. [PubMed: 23945592]
19. Urano J, Sato T, Matsuo T, Otsubo Y, Yamamoto M, Tamanoi F. Point mutations in TOR confer Rheb-independent growth in fission yeast and nutrient-independent mammalian TOR signaling in mammalian cells. Proc Natl Acad Sci U S A. 2007; 104(9):3514–9. Epub 2007/03/16. doi: 10.1073/pnas.0608510104. PubMed PMID: 17360675; PubMed Central PMCID: PMC1805553. [PubMed: 17360675]
20. Zhao JJ, Liu Z, Wang L, Shin E, Loda MF, Roberts TM. The oncogenic properties of mutant p110alpha and p110beta phosphatidylinositol 3-kinases in human mammary epithelial cells. Proc

Natl Acad Sci U S A. 2005; 102(51):18443–8. doi: 10.1073/pnas.0508988102. PubMed PMID: 16339315; PubMed Central PMCID: PMC1317954. [PubMed: 16339315]

21. Schubbert S, Shannon K, Bollag G. Hyperactive Ras in developmental disorders and cancer. Nat Rev Cancer. 2007; 7(4):295–308. Epub 2007/03/27. doi: nrc2109 [pii] 10.1038/nrc2109. PubMed PMID: 17384584. [PubMed: 17384584]
22. Network TCGAR. Comprehensive molecular characterization of clear cell renal cell carcinoma. Nature. 2013; 499(7456):43–9. Epub 2013/06/25. doi: 10.1038/nature12222. PubMed PMID: 23792563. [PubMed: 23792563]
23. Lawrence MS, Stojanov P, Mermel CH, Robinson JT, Garraway LA, Golub TR, et al. Discovery and saturation analysis of cancer genes across 21 tumour types. Nature. 2014; 505(7484):495–501. doi: 10.1038/nature12912. PubMed PMID: 24390350. [PubMed: 24390350]
24. Peterson TR, Laplante M, Thoreen CC, Sancak Y, Kang SA, Kuehl WM, et al. DEPTOR is an mTOR inhibitor frequently overexpressed in multiple myeloma cells and required for their survival. Cell. 2009; 137(5):873–86. Epub 2009/05/19. doi: S0092-8674(09)00389-4 [pii] 10.1016/j.cell.2009.03.046. PubMed PMID: 19446321; PubMed Central PMCID: PMC2758791. [PubMed: 19446321]
25. Dumont FJ, Staruch MJ, Grammer T, Blenis J, Kastner CA, Rupprecht KM. Dominant mutations confer resistance to the immunosuppressant, rapamycin, in variants of a T cell lymphoma. Cell Immunol. 1995; 163(1):70–9. Epub 1995/06/01. doi: S0008-8749(85)71100-8 [pii] 10.1006/cimm.1995.1100. PubMed PMID: 7538911. [PubMed: 7538911]
26. Efeyan A, Zoncu R, Sabatini DM. Amino acids and mTORC1: from lysosomes to disease. Trends Mol Med. 18(9):524–33. Epub 2012/07/04. doi: S1471-4914(12)00093-7 [pii] 10.1016/j.molmed.2012.05.007. PubMed PMID: 22749019; PubMed Central PMCID: PMC3432651. [PubMed: 22749019]
27. Urasaki Y, Heath L, Xu CW. Coupling of glucose deprivation with impaired histone H2B monoubiquitination in tumors. PLoS One. 7(5):e36775. Epub 2012/05/23. doi: 10.1371/journal.pone.0036775 PONE-D-12-00359 [pii]. PubMed PMID: 22615809; PubMed Central PMCID: PMC3353945. [PubMed: 22615809]
28. Hirayama A, Kami K, Sugimoto M, Sugawara M, Toki N, Onozuka H, et al. Quantitative metabolome profiling of colon and stomach cancer microenvironment by capillary electrophoresis time-of-flight mass spectrometry. Cancer Res. 2009; 69(11):4918–25. Epub 2009/05/22. doi: 0008-5472.CAN-08-4806 [pii] 10.1158/0008-5472.CAN-08-4806. PubMed PMID: 19458066. [PubMed: 19458066]
29. Gulhati P, Zaytseva YY, Valentino JD, Stevens PD, Kim JT, Sasazuki T, et al. Sorafenib enhances the therapeutic efficacy of rapamycin in colorectal cancers harboring oncogenic KRAS and PIK3CA. Carcinogenesis. 33(9):1782–90. Epub 2012/06/15. doi: bgs203 [pii] 10.1093/carcin/bgs203. PubMed PMID: 22696593; PubMed Central PMCID: PMC3514899. [PubMed: 22696593]
30. Bar-Peled L, Chantranupong L, Cherniack AD, Chen WW, Ottina KA, Grabiner BC, et al. A Tumor suppressor complex with GAP activity for the Rag GTPases that signal amino acid sufficiency to mTORC1. Science. 2013; 340(6136):1100–6. Epub 2013/06/01. doi: 10.1126/science.1232044. PubMed PMID: 23723238. [PubMed: 23723238]
31. Meric-Bernstam F, Akcakanat A, Chen H, Do KA, Sangai T, Adkins F, et al. PIK3CA/PTEN mutations and Akt activation as markers of sensitivity to allosteric mTOR inhibitors. Clinical cancer research : an official journal of the American Association for Cancer Research. 2012; 18(6):1777–89. doi: 10.1158/1078-0432.CCR-11-2123. PubMed PMID: 22422409; PubMed Central PMCID: PMC3307149. [PubMed: 22422409]
32. Shoji K, Oda K, Kashiyama T, Ikeda Y, Nakagawa S, Sone K, et al. Genotype-dependent efficacy of a dual PI3K/mTOR inhibitor, NVP-BEZ235, and an mTOR inhibitor, RAD001, in endometrial carcinomas. PLoS One. 2012; 7(5):e37431. doi: 10.1371/journal.pone.0037431. PubMed PMID: 22662154; PubMed Central PMCID: PMC3360787. [PubMed: 22662154]
33. Totary-Jain H, Sanoudou D, Dautriche CN, Schneller H, Zambrana L, Marks AR. Rapamycin resistance is linked to defective regulation of Skp2. Cancer Res. 2012; 72(7):1836–43. doi: 10.1158/0008-5472.CAN-11-2195. PubMed PMID: 22311674; PubMed Central PMCID: PMC3690511. [PubMed: 22311674]

34. Yang H, Rudge DG, Koos JD, Vaidialingam B, Yang HJ, Pavletich NP. mTOR kinase structure, mechanism and regulation. Nature. 497(7448):217–23. Epub 2013/05/03. doi: nature12122 [pii] 10.1038/nature12122. PubMed PMID: 23636326. [PubMed: 23636326]

35. Vogt PK, Hart JR, Gymnopoulos M, Jiang H, Kang S, Bader AG, et al. Phosphatidylinositol 3-kinase: the oncoprotein. Curr Top Microbiol Immunol. 347:79–104. Epub 2010/06/29. doi: 10.1007/82_2010_80. PubMed PMID: 20582532; PubMed Central PMCID: PMC2955792. [PubMed: 20582532]

36. O'Reilly KE, Rojo F, She QB, Solit D, Mills GB, Smith D, et al. mTOR inhibition induces upstream receptor tyrosine kinase signaling and activates Akt. Cancer Res. 2006; 66(3):1500–8. Epub 2006/02/03. doi: 66/3/1500 [pii] 10.1158/0008-5472.CAN-05-2925. PubMed PMID: 16452206; PubMed Central PMCID: PMC3193604. [PubMed: 16452206]

37. Sonpavde G, Choueiri TK. Precision medicine for metastatic renal cell carcinoma. Urol Oncol. Epub 2013/11/19. doi: S1078-1439(13)00301-3 [pii] 10.1016/j.urolonc.2013.07.010. PubMed PMID: 24239472.

38. Wagle N, Grabiner B, Van Allen E, Hodis E, Jacobus S, Supko J, et al. Activating mTOR mutations in a patient with an extraordinary response on a phase I trial of everolimus and pazopanib. Cancer Discovery. 2014 In press.

39. Liu Q, Chang JW, Wang J, Kang SA, Thoreen CC, Markhard A, et al. Discovery of 1-(4-(4-propionylpiperazin-1-yl)-3-(trifluoromethyl)phenyl)-9-(quinolin-3-yl)benz o[h] [1,6]naphthyridin-2(1H)-one as a highly potent, selective mammalian target of rapamycin (mTOR) inhibitor for the treatment of cancer. J Med Chem. 53(19):7146–55. Epub 2010/09/24. doi: 10.1021/jm101144f. PubMed PMID: 20860370. [PubMed: 20860370]

40. Burnett PE, Barrow RK, Cohen NA, Snyder SH, Sabatini DM. RAFT1 phosphorylation of the translational regulators p70 S6 kinase and 4E-BP1. Proc Natl Acad Sci U S A. 1998; 95(4):1432–7. Epub 1998/03/21. PubMed PMID: 9465032; PubMed Central PMCID: PMC19032. [PubMed: 9465032]

41. Sancak Y, Peterson TR, Shaul YD, Lindquist RA, Thoreen CC, Bar-Peled L, et al. The Rag GTPases bind raptor and mediate amino acid signaling to mTORC1. Science. 2008; 320(5882): 1496–501. Epub 2008/05/24. doi: 1157535 [pii] 10.1126/science.1157535. PubMed PMID: 18497260; PubMed Central PMCID: PMC2475333. [PubMed: 18497260]

Significance

We report that a diverse set of cancer-associated *MTOR* mutations confer increased mTORC1/2 pathway activity and that cells harboring these mutations are highly sensitive to rapamycin in culture and *in vivo*. These findings are clinically relevant as the *MTOR* mutations characterized herein may serve as biomarkers for predicting tumor responses to mTOR inhibitors.

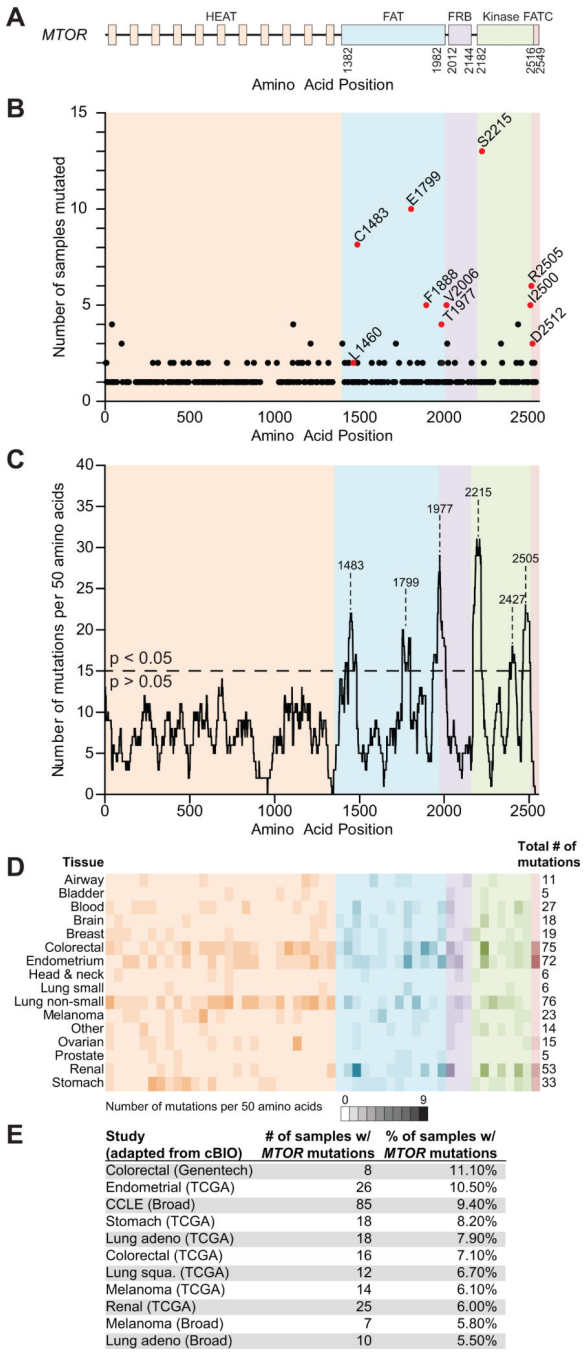

Study (adapted from cBIO)	# of samples w/ *MTOR* mutations	% of samples w/ *MTOR* mutations
Colorectal (Genentech)	8	11.10%
Endometrial (TCGA)	26	10.50%
CCLE (Broad)	85	9.40%
Stomach (TCGA)	18	8.20%
Lung adeno (TCGA)	18	7.90%
Colorectal (TCGA)	16	7.10%
Lung squa. (TCGA)	12	6.70%
Melanoma (TCGA)	14	6.10%
Renal (TCGA)	25	6.00%
Melanoma (Broad)	7	5.80%
Lung adeno (Broad)	10	5.50%

Figure 1. Cancer-associated *MTOR* mutations

1A – The domain structure of MTOR is shown.

1B – The graph indicates the number of samples with *MTOR* mutations at the indicated amino acid positions. Red colored samples were tested for pathway activation in Figure 2.

1C – A density plot of the same *MTOR* mutations from 1B identifies six distinct mutational clusters with a p-value <0.05.

1D – The number of samples with *MTOR* mutations from a given tissue types varies across the length of the gene; the intensity of color reflects the number of samples from a given cancer subtype in that region.

1E – Cancer sequencing studies with 5% or more of samples harboring *MTOR* point mutations is shown.

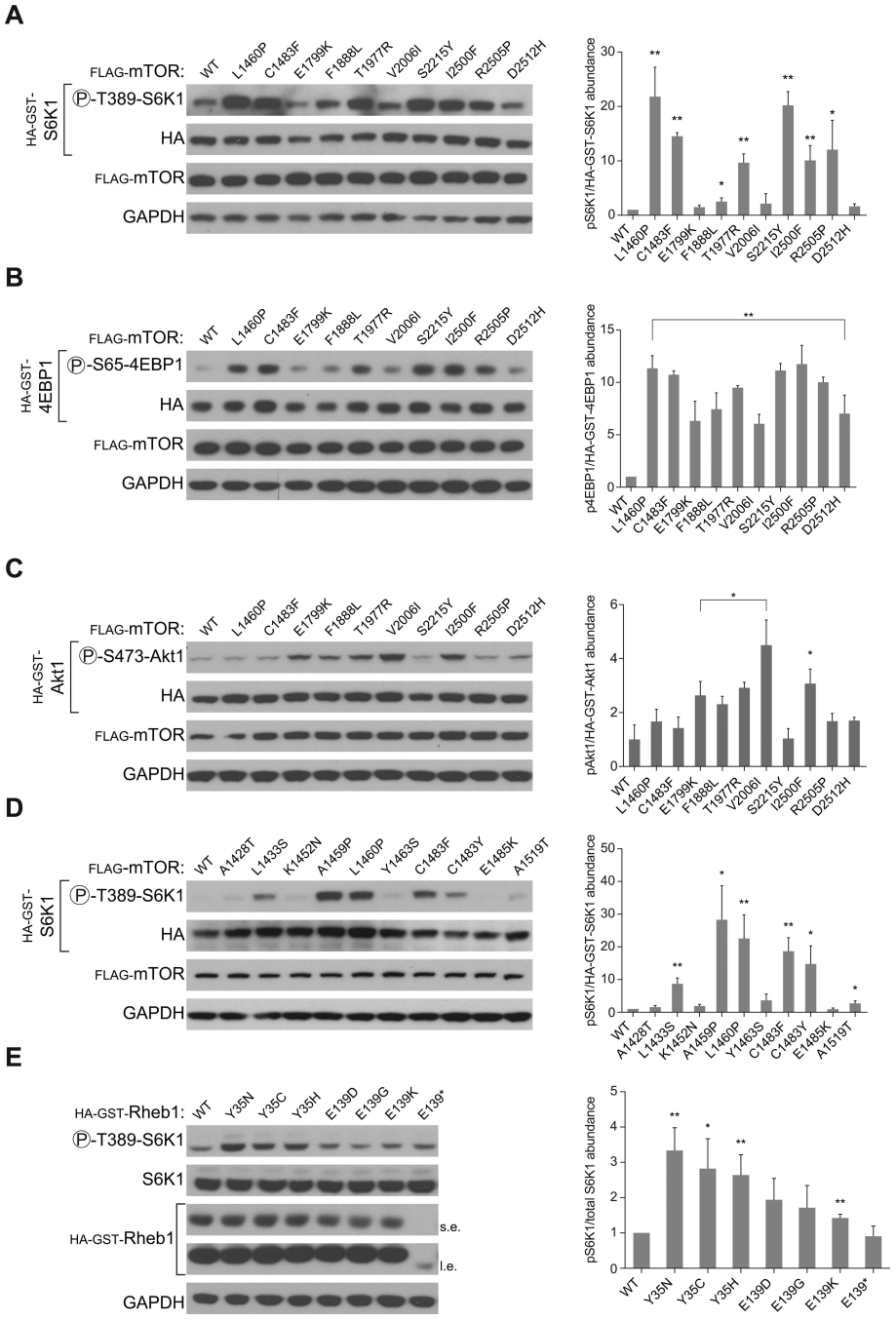

Figure 2. mTORC1 and mTORC2 activating mutations in *MTOR* and *RHEB*

2A – Several distinct mTOR mutants induce S6K1 phosphorylation. HEK-293T cells were co-transfected with HA-GST-S6K1 and mTOR WT or mutant cDNAs in expression vectors followed by whole cell lysis 48 hours after transfection. The lysates were then immunoblotted for the indicated proteins and the phosphorylation state of S6K1. Densitometry of pS6K1 vs. HA-GST-S6K1 from three separate experiments is shown on the right, the error bars represent SEM.

2B – Several distinct mTOR mutants induce 4EBP1 phosphorylation. HEK-293T cells were cotransfected with HA-GST-4EBP1 and mTOR WT or mutant cDNAs in expression vectors followed by whole cell lysis 48 hours after transfection. The lysates

were then immunoblotted for the indicated proteins and the phosphorylation state of 4EBP1. Densitometry of p4EBP1 vs. HA-GST-4EBP1 from three separate experiments is shown on the right, the error bars represent SEM.

2C – Several mTOR mutants induce Akt1 phosphorylation. HEK-293E cells were co-transfected with HAGST-Akt1 and mTOR WT or mutant cDNAs in expression vectors followed by whole cell lysis 48 hours after transfection and an overnight 0.5% serum starvation. The lysates were then immunoblotted for the indicated proteins and the phosphorylation state of Akt1. Densitometry of pAkt1 vs. HA-GST-Akt1 from three separate experiments is shown on the right, the error bars represent SEM.

2D – The C1483 cluster harbors non-recurrent mTORC1-activating mutations from kidney cancer patients. HEK-293T cells were co-transfected with HA-GST-S6K1 and mTOR WT or mutant cDNAs in expression vectors followed by whole cell lysis 48 hours after transfection. The lysates were then immunoblotted as above. Densitometry of pS6K1 vs. HA-GST-S6K1 from three separate experiments is shown on the right, the error bars represent SEM.

2E – Rheb1 mutants induce S6K1 phosphorylation. HEK-293T cells were transfected with Rheb1 WT or mutant cDNAs in expression vectors followed by whole cell lysis 48 hours after transfection. The lysates were then immunoblotted as above. Densitometry of pS6K1 vs. total S6K1 from three separate experiments is shown on the right, the error bars represent SEM.

In all cases, one asterisk indicates a p value less than 0.1, two asterisks indicates a p value less than 0.01.

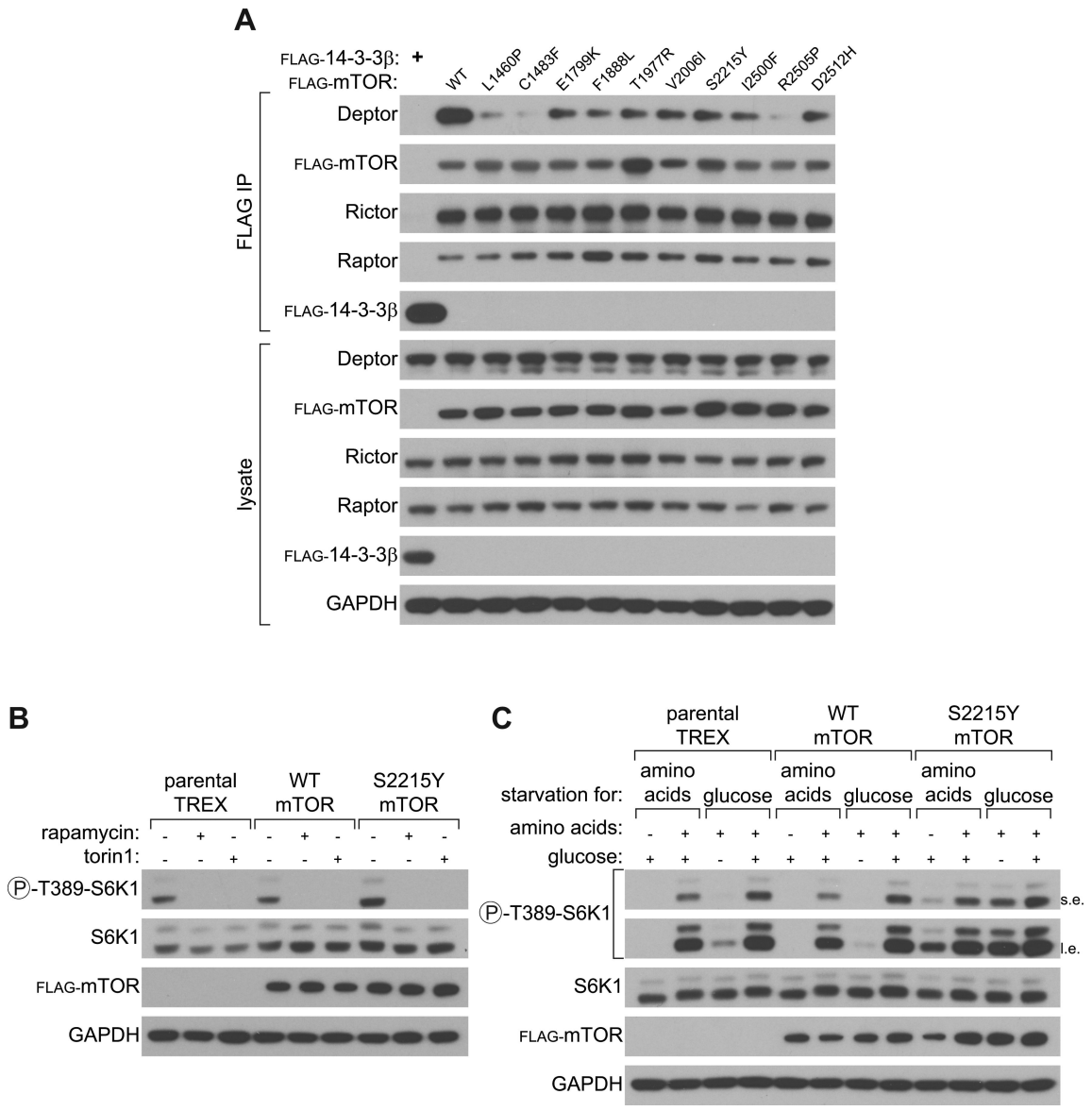

Figure 3. mTOR mutants bind less Deptor and cells expressing the mTOR S2215Y mutation are resistant to nutrient deprivation

3A – Exogenously expressed WT and mutant mTOR co-immunoprecipitate equally well endogenous Raptor and Rictor, but have reduced Deptor binding. HEK-293T cells were co-transfected with mTOR WT or mutant cDNAs in expression vectors, lysates were prepared 48 hours after transfection, and the anti-FLAG immunoprecipitates or lysates were immunoblotted for the indicated proteins.

3B – mTOR WT and S2215Y are equally sensitive to pharmacological mTOR inhibition. Parental TREX cells or those with stable expression of mTOR WT or S2215Y were treated with rapamycin or Torin1 as described in the methods. Whole cell lysates were then immunoblotted as in Figure 2.

3C – The S2215Y mTOR mutant confers resistance to nutrient deprivation on S6K1 phosphorylation. Parental TREX cells or those with stable expression of mTOR WT or S2215Y were starved and re-fed amino acids or glucose as described in the methods. Whole cell lysates were analyzed with immunoblotting as above.

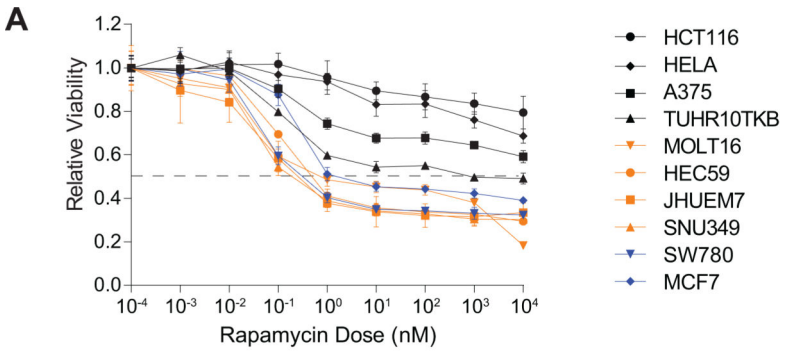

B

Cell Line	Tissue	MTOR Mutation(s)	Other Mutation(s)	Rapamycin IC50 (nM)
HCT116	Colon		CTNNB1, KRAS, PIK3CA	-
HELA	Endometrium		STK11	-
A375	Skin	R2152C	BRAF	-
TUHR10TKB	Kidney	V2006L	CDKN2A/B, EGFR, VHL	500
MOLT16	T Cell	**C1483Y**, R2430M	CDKN2A/B, TP53, MLH1	0.75
HEC59	Endometrium	R460*, **E1799K**	NF1, PTEN	0.49
JHUEM7	Endometrium	**S2215Y**	APC, NF1, PTEN	0.23
SNU349	Kidney	**E1799K**	EGFR, MLH1	0.19
SW780	Bladder		CDKN2A/B, NPRL2	0.31
MCF7	Breast		PIK3CA	1.0

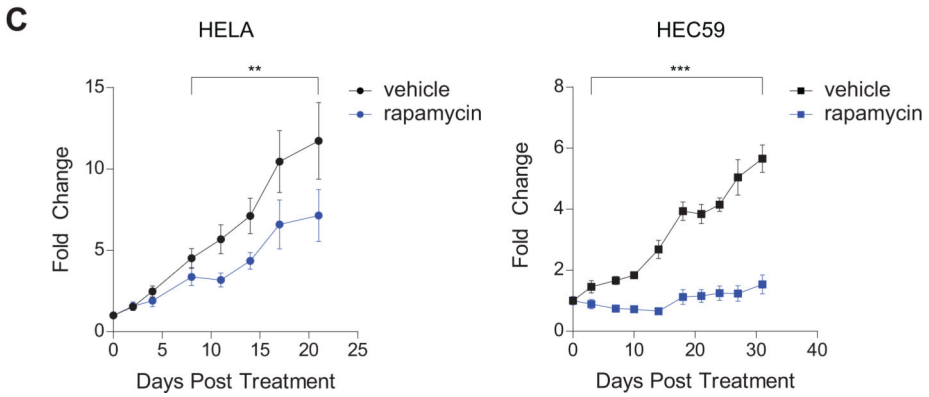

Figure 4. Rapamycin inhibits the proliferation of cancer cell lines with hyperactivating *MTOR* mutations

4A – Proliferation of multiple cancer cell lines with WT or mutant mTOR is differentially sensitive to rapamycin treatment. Cancer cell lines were seeded onto 96 well plates, treated with rapamycin 24 hours later, and cell viability was measured using Cell Titer Glo as described in the methods. Error bars indicate SD.

4B – The tissue of origin, *MTOR* mutational status, commonly mutated oncogenes/tumor suppressors and rapamycin IC50 from Figure 4A are shown for each cancer cell line.

4C – HEC59 cell xenografts are exquisitely sensitive to rapamycin treatment as compared to HeLa cell xenografts. Nine injections each of 3×10^6 HeLa or HEC59 cells were implanted subcutaneously into the flanks of eight-week-old nude mice. One week after injection, the mice were treated daily with vehicle or rapamycin and tumor size was measured for an additional three weeks. Error bars indicate SEM, two asterisks indicate p-values less than 0.05, and three asterisks indicate p-values less than 0.01.